# Expanded View Figures

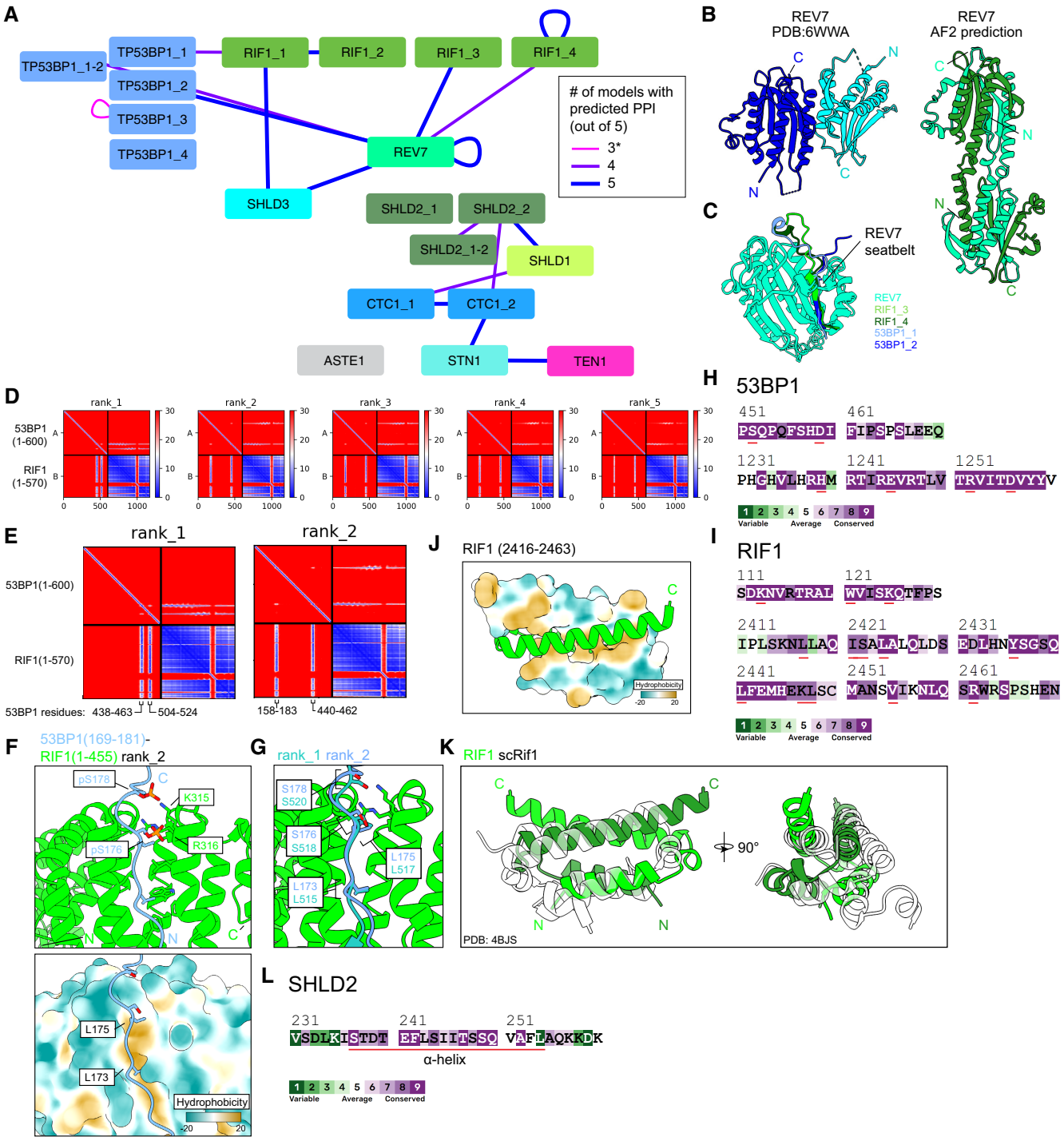


**Figure EV1.**

**Figure EV1. Data supporting the AlphaFold2-Multimer pairwise matrix screen for protein–protein interactions in the 53BP1-RIF1-shieldin-CST pathway.**

A Schematic of predictions that meet the cutoff scores of pDockQ > 0.23, interface PAE < 15 Å, and four or more repeated predictions. Nodes are proteins and fragments used for each prediction. Junction nodes are fragments spanning ± 200 residues from where large proteins are divided and are only shown if interactions meeting the score cutoffs are present (e.g., TP53BP1_1-2). Edges link the two chains used for each prediction. Edge thickness and color correspond to the number of predictions (out of five for each pair) meeting the score cutoffs. *Self-association of TP53BP1_3 is shown despite not meeting the ≥ 4 consistent model cutoff due to previous experimental results corroborating the predicted interaction.
B Comparison of REV7 dimer structures determined from X-ray crystallography (Left, PDB ID: 6WWA) and from AlphaFold2 prediction (right).
C Superimposition of predicted heterodimeric structures between REV7 and RIF1 fragments 3 and 4 and 53BP1 fragments 1 and 2. See also Appendix Fig S1.
D PAE plots of the predicted 53BP1 (fragment 1; 1–600) and RIF1 (fragment 1; 1–570), ranked by predicted template model (pTM) scores.
E Close-ups of two PAE plots from (D), with the 53BP1 regions of high PAE confidence labeled.
F Predicted structures of the 53BP1-RIF1 interface. Top, phosphate groups modeled onto two serines of 53BP1 whose phosphorylation is known to be essential for interaction with RIF1. Bottom, surface representation of RIF1 colored by hydrophobicity.
G Superimposition of the 53BP1-RIF1 interface from two different predicted models.
H ConSurf sequence conservation analysis of the indicated 53BP1 regions. Residues important for the predicted secondary RIF1-53BP1 interface (53BP1 residues 440–462) or 53BP1 oligomerization (53BP1 residues 1,237–1,286) are underlined in red.
I ConSurf sequence conservation analysis of the indicated RIF1 regions. Residues important for the predicted RIF1 oligomerization (RIF1 residues 2,435–2,464) or the predicted secondary RIF1-53BP1 interface (RIF1 residues 79–169) are underlined in red.
J Predicted structure of the RIF1 dimerization interface, one monomer is shown with surface representation colored by hydrophobicity.
K Superimposition of the RIF1 oligomerization domain and the experimentally-determined structure (translucent) of the corresponding region in *S. cerevisiae* Rif1 (PDB ID: 4BJS).
L ConSurf sequence conservation analysis of the indicated SHLD2 region. Residues comprising the alpha helix predicted to bind SHLD2 OB-A and OB-B are underlined in red.

**Figure EV2. Data supporting the SHLD3 C terminus as necessary and sufficient for RIF1 binding and recruitment to sites of DNA damage.**

A Top-ranking model of RIF1 (1–615) and SHLD3 (131–250) colored by pLDDT score.
B Five AF2-predicted models of RIF1 (1–615) and SHLD3 (131–250) superimposed, aligned by the SHLD3 chain.
C Top-ranking AF2 model of RIF1 (1–615) and SHLD3 (131–250), highlighting residues associated with SHLD3 DNA binding and RIF1 53BP1 phosphopeptide binding.
D Scatter plot of interface PAE vs pDockQ scores of AF2-predicted models between RIF1 (1–615) with the indicated paralogues of the SHLD3 eIF4E-like domain. Cutoff scores of 15 Å and 0.23 PAE and pDockQ scores are shown as dotted lines. Models meeting the cutoff are represented as black points and those that do not are represented as gray points.
E Immunoblot of whole cell extracts of U2OS 2-6-3 cells transfected with plasmids encoding the indicated eGFP-tagged SHLD3. Lysates were probed for eGFP and tubulin (loading control). IB—immunoblot. EV—empty vector.
F Representative micrographs of the LacR/LacO assay using mCherry-LacR as bait to evaluate chromatin recruitment of eGFP-tagged SHLD3 variants as a control for the experiments using mCherry-LacR-RIF1$^{N}$ in Fig 2E and F.
G Quantification of F. GFP intensities are presented as a ratio between the average fluorescence intensity within the mCherry-labeled LacR focus and the average nuclear intensity. Bars represent mean ($n$ = 140, 138, 131, 133 for eGFP, eGFP-SHLD3, eGFP-SHLD3$^{N}$, eGFP-SHLD3$^{C}$ from three biologically independent experiments).
H Representative micrographs of control experiments for the LacR-FokI assay in Fig 2H and I to evaluate DNA-damage recruitment of eGFP-tagged SHLD3 variants. LacR-FokI expression was not induced, and no mCherry-LacR-FokI or eGFP-SHLD3 foci were detected.
I Representative micrographs of the LacR-FokI assay to evaluate DNA-damage induction after mCherry-LacR-FokI expression. U2OS 2-6-3 cells were transfected with plasmids encoding eGFP-SHLD3 and treated with 4-hydroxytamoxifen and Shield-1 peptide to induce mCherry-LacR-FokI expression. The cells were then analyzed for γ-H2AX focus formation colocalizing with mCherry-LacR-FokI as a proxy for DNA double-strand break formation through immunofluorescence (top). Colocalization of mCherry-LacR-FokI focus with endogenous RIF1 was also assessed (bottom).
J Quantification of I. Immunofluorescence intensities are presented as a ratio between the average fluorescence intensity within the mCherry-labeled LacR focus and the average nuclear intensity. Bars represent mean ($n$ = 95, 88, 90, 94 for γ-H2AX eGFP, γ-H2AX eGFP-SHLD3, RIF1 eGFP, RIF1 eGFP-SHLD3 from two biologically independent experiments).

Source data are available online for this figure.

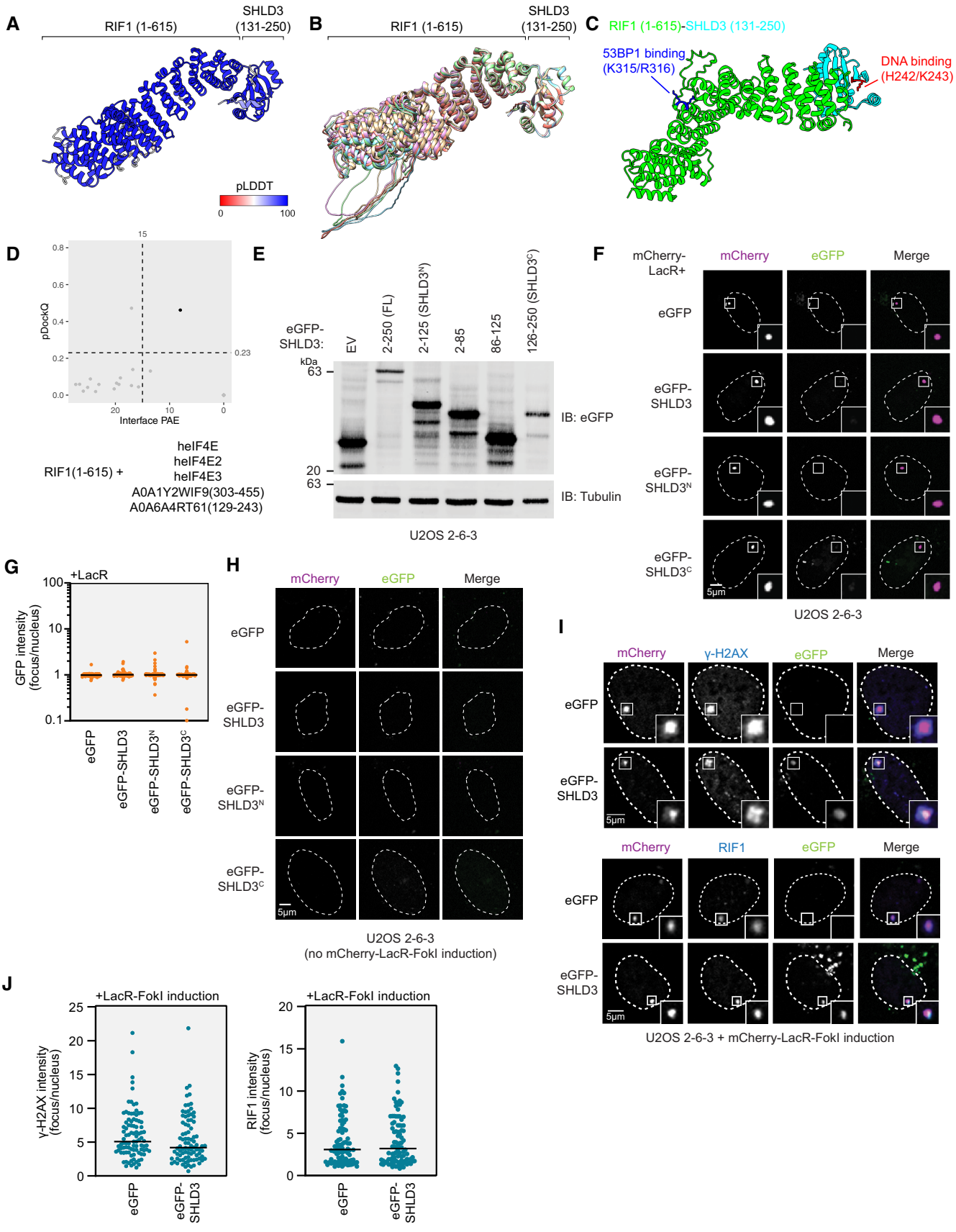


**Figure EV2.**

**Figure EV3. Data supporting the polar interactions that are essential for SHLD3-RIF1 binding.**

A Immunoblot of whole cell extracts of U2OS 2-6-3 cells transfected with plasmids encoding the indicated eGFP-tagged SHLD3$^{C}$ (residues 126–250) variants. Lysates were probed for eGFP and tubulin (loading control). IB—immunoblot. EV—empty vector. WT—wild-type.

B Representative micrographs of the LacR/LacO assay using mCherry-LacR-RIF1$^{N}$ as bait to evaluate chromatin recruitment of eGFP-tagged SHLD3$^{C}$ alanine substitution variants shown in Fig 3C. SHLD3$^{C}$: residues 126–250. RIF1$^{N}$: residues 1–967.

C Representative micrographs of the LacR-FokI assay to evaluate DNA-damage recruitment of eGFP-tagged SHLD3$^{C}$ alanine substitution variants after induction of LacR-FokI expression shown in Fig 3D. SHLD3$^{C}$: residues 126–250.

D Representative micrographs of the LacR-FokI assay to evaluate DNA-damage recruitment of endogenous RIF1 after induction of LacR-FokI expression in the presence of exogenously expressed eGFP-tagged SHLD3$^{C}$ alanine substitution variants. SHLD3$^{C}$: residues 126–250.

E Quantification of D. RIF1 immunofluorescence intensities are presented as a ratio between the average fluorescence intensity within the mCherry-labeled LacR focus and the average nuclear intensity. Bars represent mean values ($n = 99, 92, 88, 97, 90, 92, 100$ for EV, WT, S131A, W132A, R166A, N201A, D216A from two biologically independent experiments).

F Immunoblot of whole cell extracts of U2OS 2-6-3 cells transfected with plasmids encoding the indicated eGFP-tagged SHLD3$^{C}$ (residues 126–250) variants. Lysates were probed for eGFP and tubulin (loading control).

G Representative micrographs of the LacR/LacO assay using mCherry-LacR-RIF1$^{N}$ as bait to evaluate chromatin recruitment of eGFP-tagged SHLD3 H242A/K243A.

H Quantification of G. GFP intensities are presented as a ratio between the average fluorescence intensity within the mCherry-labeled LacR-RIF1$^{N}$ focus and the average nuclear intensity. Bars represent mean values ($n = 127, 129, 136$ for EV, WT, H242A/K243A from three biologically independent experiments). Analysis was performed using the Kruskal–Wallis test followed by Dunn's multiple comparisons against empty vector control. ****$P < 0.0001$.

I Immunoblot of whole cell extracts of RPE *SHLD3-KO* cells stably transduced with lentivirus encoding the indicated 3xFLAG-tagged SHLD3 alanine substitution variants. Lysates were probed for FLAG and tubulin (loading control). IB—immunoblot.

J Immunoblot of whole cell extracts of complemented RPE *SHLD3-KO* cells shown in (I) that were transfected with plasmid encoding eGFP-SHLD2. Lysates were probed for eGFP and tubulin (loading control).

Source data are available online for this figure.

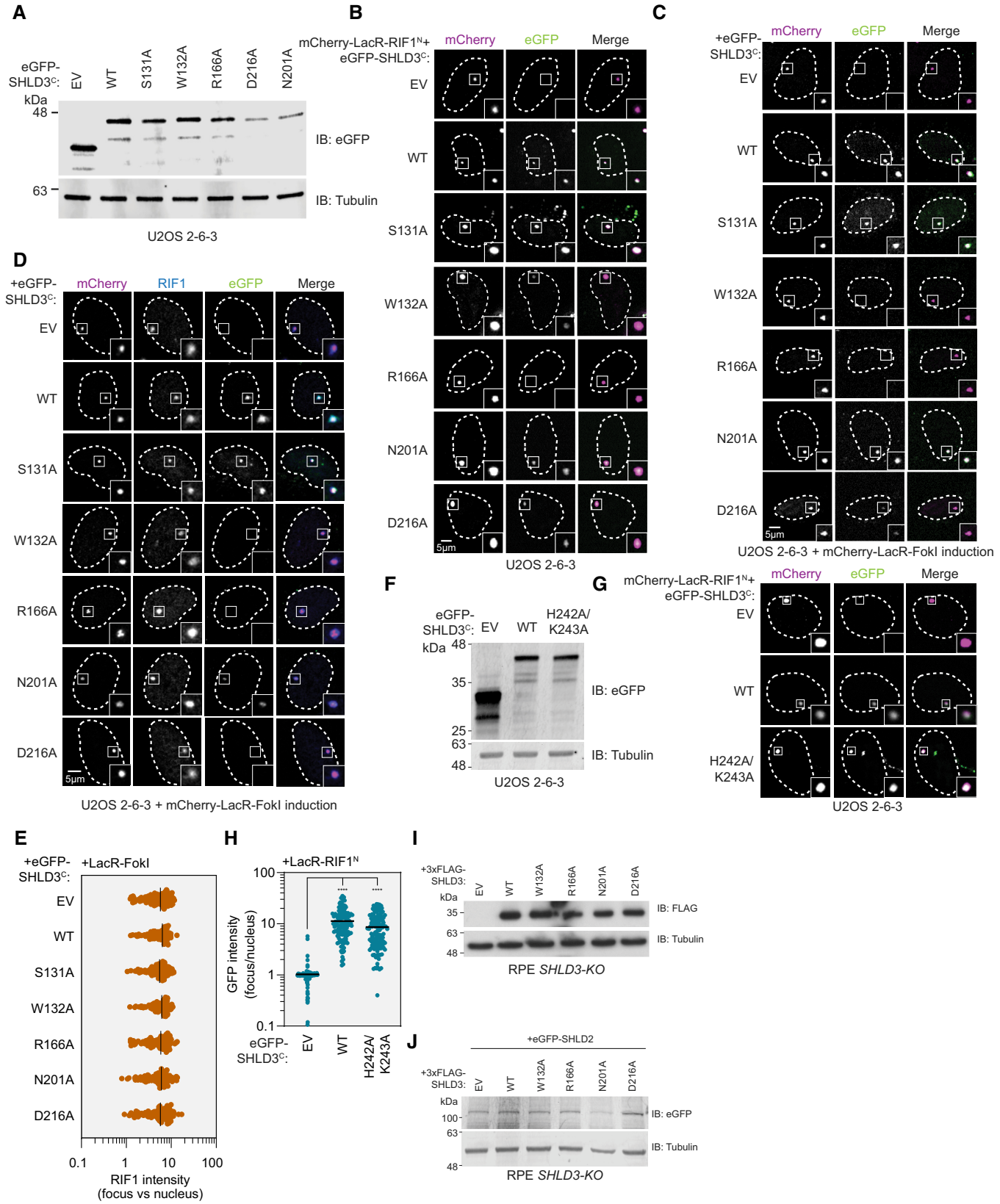


**Figure EV3.**

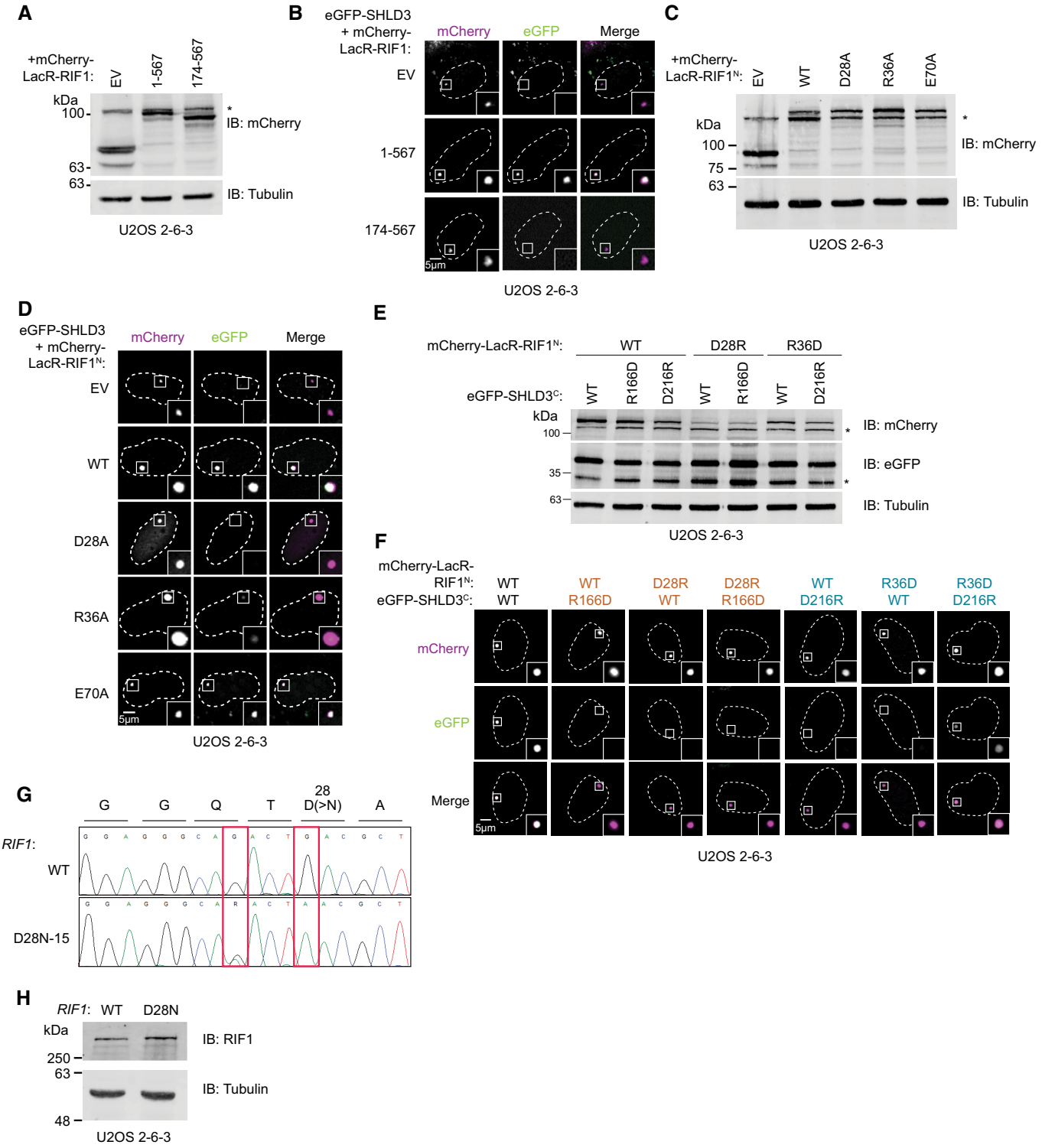
A
+mCherry-LacR-RIF1:
EV
1-567
174-567
kDa
100
63
63
IB: mCherry
IB: Tubulin
U2OS 2-6-3
B
eGFP-SHLD3 + mCherry-LacR-RIF1:
mCherry
eGFP
Merge
EV
1-567
174-567
5µm
U2OS 2-6-3
C
+mCherry-LacR-RIF1N:
EV
WT
D28A
R36A
E70A
kDa
100
75
63
IB: mCherry
IB: Tubulin
U2OS 2-6-3
D
eGFP-SHLD3 + mCherry-LacR-RIF1N:
mCherry
eGFP
Merge
EV
WT
D28A
R36A
E70A
5µm
U2OS 2-6-3
E
mCherry-LacR-RIF1N:
WT
D28R
R36D
eGFP-SHLD3C:
WT
R166D
D216R
WT
R166D
WT
D216R
kDa
100
35
63
IB: mCherry
IB: eGFP
IB: Tubulin
U2OS 2-6-3
F
mCherry-LacR-RIF1N:
eGFP-SHLD3C:
WT
WT
WT
R166D
D28R
WT
D28R
R166D
WT
D216R
R36D
WT
R36D
D216R
mCherry
eGFP
Merge
5µm
U2OS 2-6-3
G
G
G
Q
T
28
D(>N)
A
RIF1:
WT
D28N-15
H
RIF1:
WT
D28N
kDa
250
63
48
IB: RIF1
IB: Tubulin
U2OS 2-6-3

**Figure EV4.**

**Figure EV4. Data supporting the extreme N terminus of RIF1 binding SHLD3 through polar residues.**

A Immunoblot of whole cell extracts of U2OS 2-6-3 cells transfected with plasmids encoding the indicated mCherry-LacR-fused RIF1 truncations. Lysates were probed for mCherry and tubulin (loading control). IB: immunoblot, EV: empty vector. *: nonspecific band.

B Representative micrographs (of three biologically independent experiments) of the LacR/LacO assay using the indicated mCherry-LacR-fused RIF1 variants to evaluate their ability to recruit eGFP-SHLD3 to chromatin shown in Fig 5A.

C Immunoblot of whole cell extracts of U2OS 2-6-3 cells transfected with plasmids encoding the indicated mCherry-LacR-fused $RIF1^{N}$ (residues 1–967) alanine variants. Lysates were probed for mCherry and tubulin (loading control). *: nonspecific band.

D Representative micrographs (of three biologically independent experiments) of the LacR/LacO assay using the indicated mCherry-LacR-fused $RIF1^{N}$ variants to evaluate their ability to recruit eGFP-SHLD3 to chromatin shown in Fig 5B. WT: wild-type.

E Immunoblot of whole cell extracts of U2OS 2-6-3 cells transfected with plasmids encoding the indicated mCherry-LacR-$RIF1^{N}$ and eGFP-$SHLD3^{C}$ variants. Lysates were probed for mCherry, eGFP, and tubulin (loading control). *: nonspecific band.

F Representative micrographs of the LacR/LacO assay using the indicated mCherry-LacR-$RIF1^{N}$ and eGFP-$SHLD3^{C}$ variants to evaluate their colocalization at LacO arrays shown in Fig 5D.

G Sanger sequencing chromatograms of PCR products amplified from U2OS 2-6-3 cells with and without subjecting it to base editing to introduce endogenous D28N mutations. A single clone was isolated that contained the desired mutation (D28N-15). Red boxes highlight induced mutations. The first heterozygous G > A mutation is silent. The second homozygous G > A mutation results in the desired D28N substitution.

H Immunoblot of whole cell extracts of U2OS 2-6-3 cells with or without base editing to introduce endogenous D28N mutation. Lysates were probed for RIF1 and tubulin (loading control).

Source data are available online for this figure.

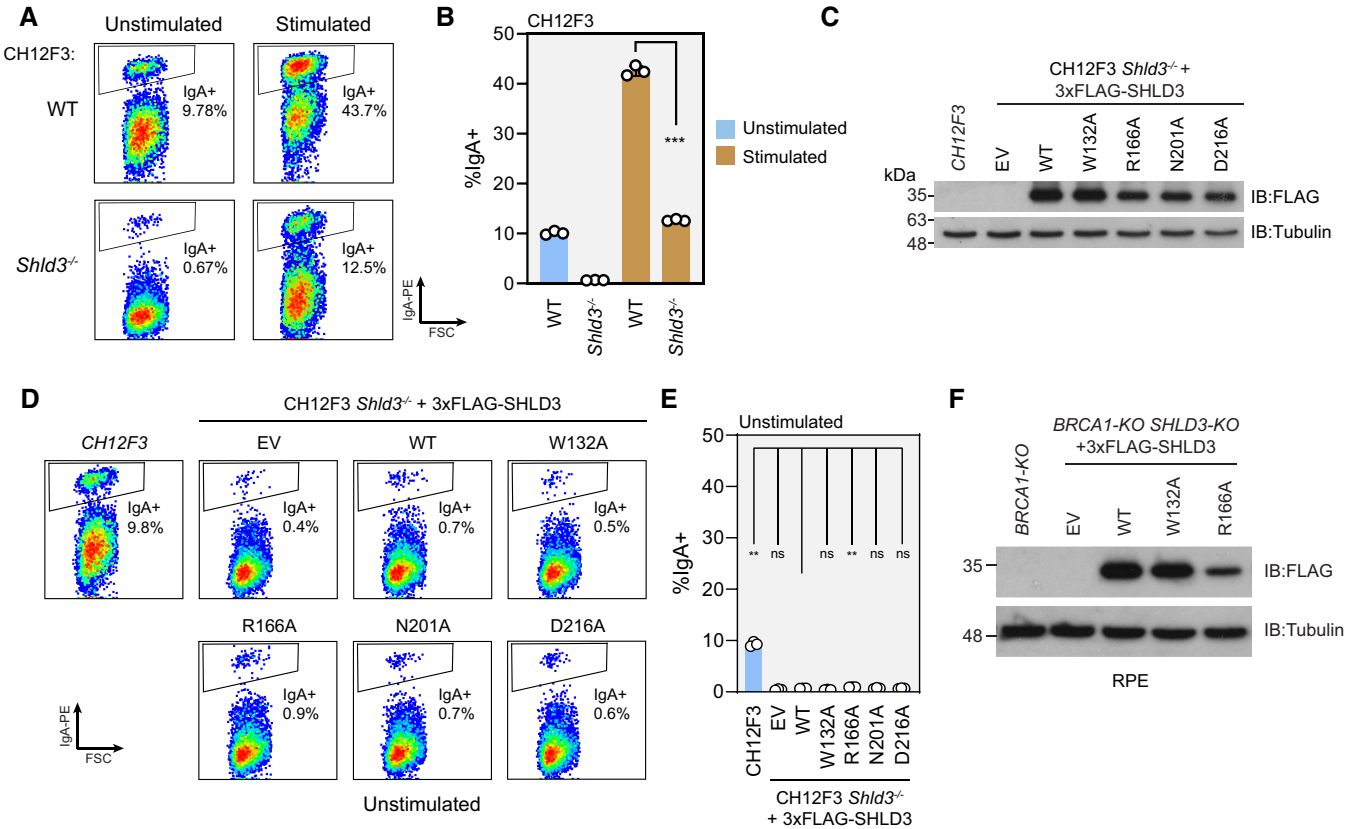


**Figure EV5.**

**Figure EV5. Data supporting the importance of SHLD3-RIF1 binding for shieldin activity.**

A Representative flow cytometry density plots measuring IgA expression in unstimulated and stimulated CH12F3 wild-type or *Shld3*$^{-/-}$ cells. Values shown are %IgA$^{+}$ cells. FSC: forward scatter. WT—wild-type.

B Quantification of class switch recombination data shown in (A). Bars represent mean ± s.d., $n = 3$ biologically independent experiments. Analysis was performed using the Welch's two-tailed *t*-test. ***$P = 0.0002$.

C Immunoblot of whole cell extracts of CH12F3 *Shld3*$^{-/-}$ cells stably transduced with lentivirus encoding the indicated FLAG-tagged SHLD3 alanine substitution variants. Lysates were probed for FLAG and tubulin (loading control). IB—immunoblot. EV—empty vector.

D Representative flow cytometry density plots measuring IgA expression in unstimulated CH12F3 wild-type or *Shld3*$^{-/-}$ cells stably transduced with lentivirus encoding FLAG-tagged SHLD3 alanine substitution variants. Control experiment for Fig 6B. Values shown are %IgA$^{+}$ cells.

E Quantification of class switch recombination data shown in (D). Bars represent mean ± s.d., $n = 3$ biologically independent experiments. Analysis was performed using the Dunnett's multiple comparisons test compared against *Shld3*$^{-/-}$ cells complemented with wild-type SHLD3. **$P < 0.01$, $^{ns}P > 0.05$.

F Immunoblot of whole cell extracts of RPE *BRCA1-KO SHLD3-KO* cells stably transduced with lentivirus encoding the indicated FLAG-tagged SHLD3 alanine substitution variants. Lysates were probed for FLAG and tubulin (loading control).

Source data are available online for this figure.